J Mater Sci: Mater Electron (2016) 27:11495–11501
DOI 10.1007/s10854-016-5277-8

Electrical properties of sol–gel derived Mg-doped Al_2O_3 films

Yong Peng[1] · Manwen Yao[1] · Ruihua Xiao[1] · Xi Yao[1]

Received: 12 April 2016 / Accepted: 28 June 2016 / Published online: 7 July 2016

Abstract Highly homogeneous and dense Mg-doped Al_2O_3 films were prepared using sol–gel method. Similar trends occur in the current–voltage characteristics of $Al_{1-x}Mg_xO_{3-\delta}$ series (x = 0, 0.5, 2 and 10 %) films, while 7.7 and 33.3 % Mg-doped Al_2O_3 films exhibit different trends, and the 33.3 % Mg-doped Al_2O_3 films have the lowest leakage current, which almost linearly increases with the applied voltage. The dielectric strength of the $Al_{1-x}Mg_xO_{3-\delta}$ series (x = 0.5, 2 and 10 %) films are slightly lower than that of undoped Al_2O_3 films, while the 7.7 and 33.3 % Mg-doped Al_2O_3 films possess higher dielectric strength than the undoped Al_2O_3 films. The Ohmic conduction dominates the leakage current of $Al_{1-x}Mg_xO_{3-\delta}$ (x = 0, 7.7 and 33.3 %) films under lower electric field, while the space-charge-limited-current and Schottky emission, and even other conduction mechanisms, could co-exist under higher electric field.

1 Introduction

Naturally abundant Alumina (Al_2O_3) is a technically important material with excellent dielectric properties, chemical and thermal stability as well as the strong adhesion to various materials [1, 2]. As an insulating material, Al_2O_3 films are widely used as gate oxides, buffer layers and other electronic circuit elements. At present, Al_2O_3 has also drawn increasing attention to explore its potential applications in high energy storage density capacitors because of the relatively high dielectric strength, large permittivity and broad band gap [3]. In general, the energy density can be described for linear dielectric by $U = 0.5\varepsilon_0\varepsilon_r E^2$, where ε_0, ε_r and E are the vacuum dielectric constant, the dielectric constant and the dielectric strength, respectively. Therefore, large dielectric constant and dielectric strength are highly desired for high energy density. In addition, the leakage current is also a key factor influencing the efficiency of energy storage, what's more, the reliability of electric devices is closely related to leakage current. According to the previous report [4], the dielectric strength of Al_2O_3 films prepared by sol–gel is only about 3 MV/cm.

In general, the electric properties of the films is determined by both extrinsic (process-related) and intrinsic factors. As for the former, efforts have been made to improve the electric properties, one is to eliminate flaws by optimizing the deposition conditions and the other is to avoid electric field concentrations of films edges by post deposition annealing. The latter focused on the relationship between the microstructure and electric properties of films. Incorporation of a fraction of additives into films is usually considered as an effective approach to improve the electric properties by eliminating or passivating the defects of the films. In the previous literatures, Dover reported the incorporation of lanthanide into TiO_2 dielectric film is able to increase the breakdown voltage and decrease the leakage current [5]. Other literatures revealed the incorporation of foreign cations (such as Ti, Y, W and Nb) into tantalum oxide films can also improve its electric properties [6–8]. In our previous report [9], the effect of titanium doping on the leakage current and breakdown characteristics of

✉ Manwen Yao
yaomw@tongji.edu.cn

Yong Peng
pengyong19872006@163.com

[1] Functional Materials Research Laboratory, School of Materials Science and Engineering, Tongji University, Shanghai 200092, China

amorphous Al_2O_3 films have been studied. The enhancement of dielectric strength of the Al_2O_3 films may be ascribed to the reducing of oxygen vacancies which are suppressed by the titanium doping. To study the effect of oxygen vacancies on the dielectric strength of Al_2O_3 films, Mg^{2+} is incorporated into Al_2O_3 films, which can effectively motivate the formation of oxygen vacancy.

In this study, the $Al_{1-x}Mg_xO_{3-\delta}$ series (x = 0, 0.5, 2 and 10 %) films have been prepared by sol–gel technology. On the other hand, as we all know, there exist two special species of magnesium-aluminum oxides: $MgAl_{12}O_{19}$ magnetoplumbite type and $MgAl_2O_4$ spinel type. Therefore, it would be significantly meaningful to compare the electrical characteristics between the $Al_{1-x}Mg_xO_{3-\delta}$ (x = 0, 0.5, 2 and 10 %) series and the stoichiometric magnesium–aluminum oxides. The emphasis of this work is placed on the current-voltage characteristics, dielectric strength, conduction mechanisms and dielectric properties of the $Al_{1-x}Mg_xO_{3-\delta}$ series films. In addition, the surface roughness and surface morphology of $Al_{1-x}Mg_xO_{3-\delta}$ series films were also investigated in this study.

2 Experimental procedure

The Mg-doped Al_2O_3 films were prepared by sol–gel technique. The reagent-grade Aluminum isopropoxide and magnesium acetate were weighed to form the composition $Al_{1-x}Mg_xO_{3-\delta}$ series (x = 0, 0.5, 2, 7.7, 10 and 33.3 %), the mixture was dissolved in 50 ml glycol ether and stirred for 30 min in an open beaker. When the mixture was heated to 90 °C, 0.02 mol acetylacetone was added to control the rate of hydrolyze, and the mixture was stirred for another 30 min. Then the solution was catalyzed with 10 ml acetic acid. After stirring 30 min and cooling down to room temperature, then a clear and transparent sol was obtained. The concentration of the obtained sol was adjusted to about 0.33 M.

After aging for 3 days, the precursor was used to deposit films on Pt/Ti/SiO_2/Si substrates (1.2 × 1.2 cm^2). The substrates were ultrasonically cleared beforehand in acetone, deionized water and ethyl alcohol, in sequence. The films were made by multiple spin coating process using a custom-made spin coater in a clean-room environment with a spin speed of 3000 rpm for 20 s for each layer. After each coating layer, the samples were baked at 70, 150, 250 and 420 °C for 5 min respectively to evaporate residual solvents. After 7 layers of coating were deposited, all the samples were annealed at 450 °C for 3 h in the furnace. To measure the electrical properties, Au electrodes with a diameter of 1 mm were deposited through a shadow mask on the top surface of the films to form MIM configuration.

The surface and cross-sectional morphology of the films were examined using a Field Emission Scanning Electron Microscope (FESEM, XL30, FEI). The micro-morphology and roughness of the films was studied using Atomic Force Microscopy (AFM, Dimension Icon, NanoScope V, Bruker). The electrical properties of the Mg-doped Al_2O_3 films were characterized by the current-voltage curves, conduction mechanism, dielectric strength and dielectric constant. The current–voltage (I–V) measurement was performed through a computer-controlled Keithley 2400 voltage source with a ramping step of 0.2 V. In this work, the Au electrode was consistently biased positively with respect to the bottom Pt electrode. The dielectric constant was measured using an Agilent 4284A LCR meter controlled by a computer.

3 Results and discussion

Figure 1 shows the AFM images of 0, 0.5 % (AM-0.5), 2 % (AM-2), 7.7 % (AM-7.7), 10 % (AM-10) and 33.3 % (AM-33.3) Mg-doped Al_2O_3 films on Pt/Ti/SiO_2/Si substrates, respectively. All films exhibit almost similar surface morphology with dense, uniform microstructure. The surfaces of undoped and Mg-doped Al_2O_3 films were analyzed by calculating the root mean square roughness of the films. The calculated results are listed in Table 1. Apart from the roughness of AM-7.7 film slightly higher than the other, there is no obvious change in roughness of the other films.

Figure 2 displays the FESEM images of undoped and Mg-doped Al_2O_3 films on Pt/Ti/SiO_2/Si substrates. As shown in Fig. 2a, b, it can be seen that the films are highly homogeneous and dense without pinholes or micro-cracks. Meanwhile, no obvious grains occur in surface or cross-section micrograph of all films, which suggest that all the films annealed at 450 °C keep amorphous. The XRD patterns also verify the above result (not shown here), which is consistent with our previous reports [10]. From the cross-section micrograph, the thickness of the films can be measured. The thickness of $Al_{1-x}Mg_xO_{3-\delta}$ (x = 0, 0.5, 2, 7.7, 10 and 33.3 %) films are 217, 207, 196, 194, 188 and 157 nm, respectively.

The current–voltage (I–V) dependence of $Al_{1-x}Mg_xO_{3-\delta}$ films is illustrated in Fig. 3. Though the leakage current of AM-10 films is slightly smaller than that of undoped Al_2O_3 films, on the whole, the similar trend occurs in the I–V curves of $Al_{1-x}Mg_xO_{3-\delta}$ (x = 0, 0.5, 2 and 10 %) films. Compared with the above $Al_{1-x}Mg_xO_{3-\delta}$ (x = 0, 0.5, 2 and 10 %) films, the AM-7.7 and AM-33.3 films exhibit different shape in the I–V curves. As for the AM-7.7 films, the leakage current increases sharply at the applied voltage above 25 V, and the leakage current is significantly higher than the others. For the AM-33.3 films, the leakage current increases almost linearly with the applied voltage, and the AM-33.3 films have the lowest

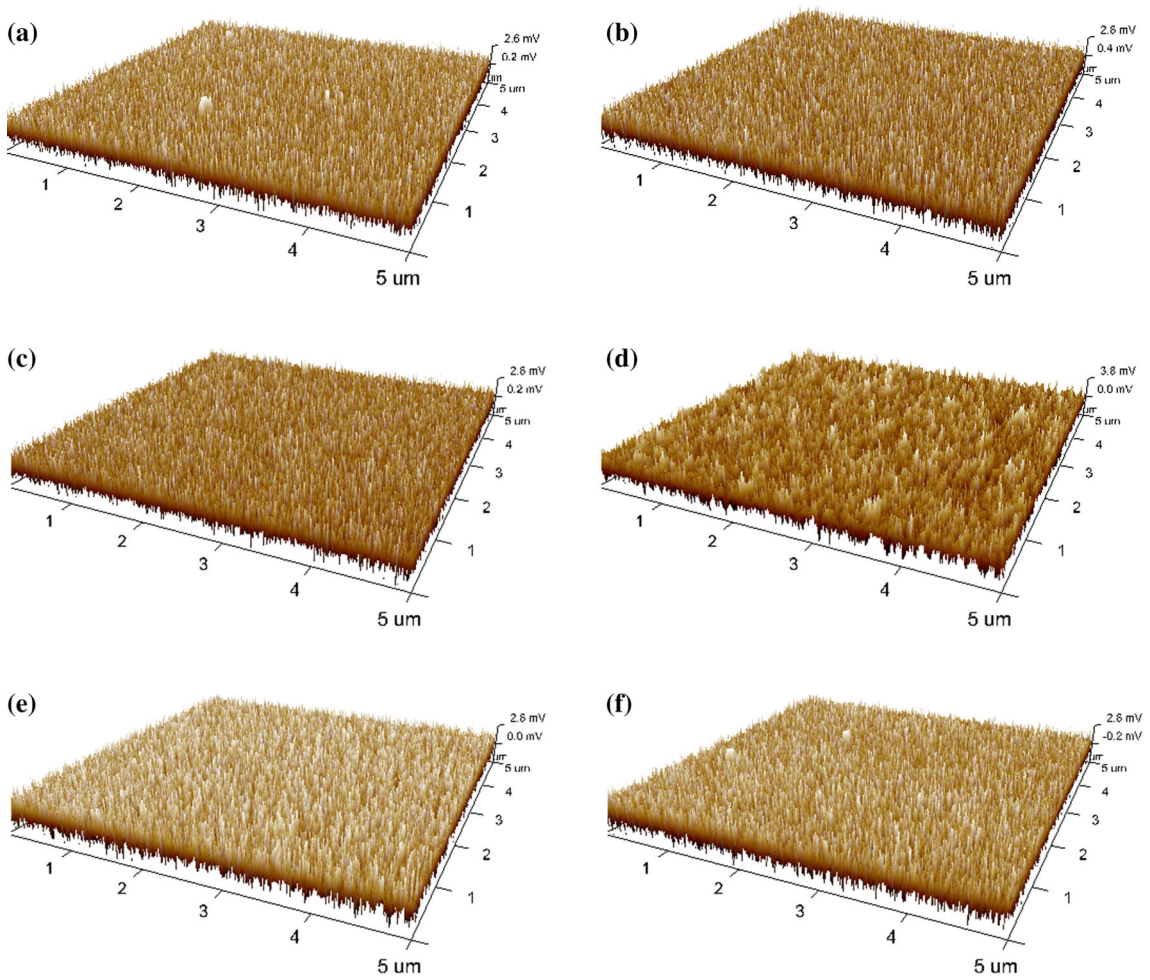

Fig. 1 Surface AFM images of $Al_{1-x}Mg_xO_{3-\delta}$ films deposited on Pt/Ti/SiO_2/Si substrates: Al_2O_3 films (**a**); AM-0.5 films (**b**); AM-2 films (**c**); AM-7.7 films (**d**); AM-10 films (**e**) and AM-33.3 films (**f**)

Table 1 Surface roughness of $Al_{1-x}Mg_xO_{3-\delta}$ films on Pt/Ti/SiO_2/Si substrates

Mg/(Mg+Al) (%)	0	0.5	2	7.7	10	33.3
Roughness (nm)	2.57	2.68	2.43	3.63	2.65	2.63

leakage current than the others at lower voltage (<30 V). The above leakage current characteristic may be closely related to the lattice structure of the films. In general, the amorphous materials possess low degree of order within the long-range scope because the atoms lack definite periodic arrangements. But within the short-range scope, the atoms in amorphous materials are arranged in a lattice-like structure. All the films keep amorphous structure in this study. For AM-7.7 and AM-33.3 films, there exist trends to form potential magnetoplumbite structure ($MgAl_{12}O_{19}$) and spinel structure ($MgAl_2O_4$) within the short-range scope, respectively. Therefore the leakage current of AM-7.7 and AM-33.3 films are different with the others. The fluctuations in the I–V curves of all the films are also observed in Fig. 3. As reported in the early literature [11], the fluctuations of leakage current indicate the occurrence of soft breakdown.

Generally, the leakage current in dielectric films at high electric field is determined to be Poole-Frenkel (PF) emission, Schottky emission (SE) or space-charge-limited-current (SCLC) [12]. In the case of Poole-Frenkel emission, it is well known as bulk limited conduction mechanism, the leakage current is generated by the field strengthened thermal excitation of trapped charges into conduction band, the Pool–Frenkel conductivity is presented by [12]

$$J_{PF} = \sigma_0 E \cdot \exp -[(E_I - \beta_{PF}E^{1/2})/kT], \quad (1)$$

where $\beta_{PF} = (q^3/\pi\varepsilon_0\varepsilon_r)^{1/2}$, σ_0 is the sample-dependent zero-field conductivity, k the Boltzmann constant, T the temperature (in Kelvin), q the electron charge, ε_0 the

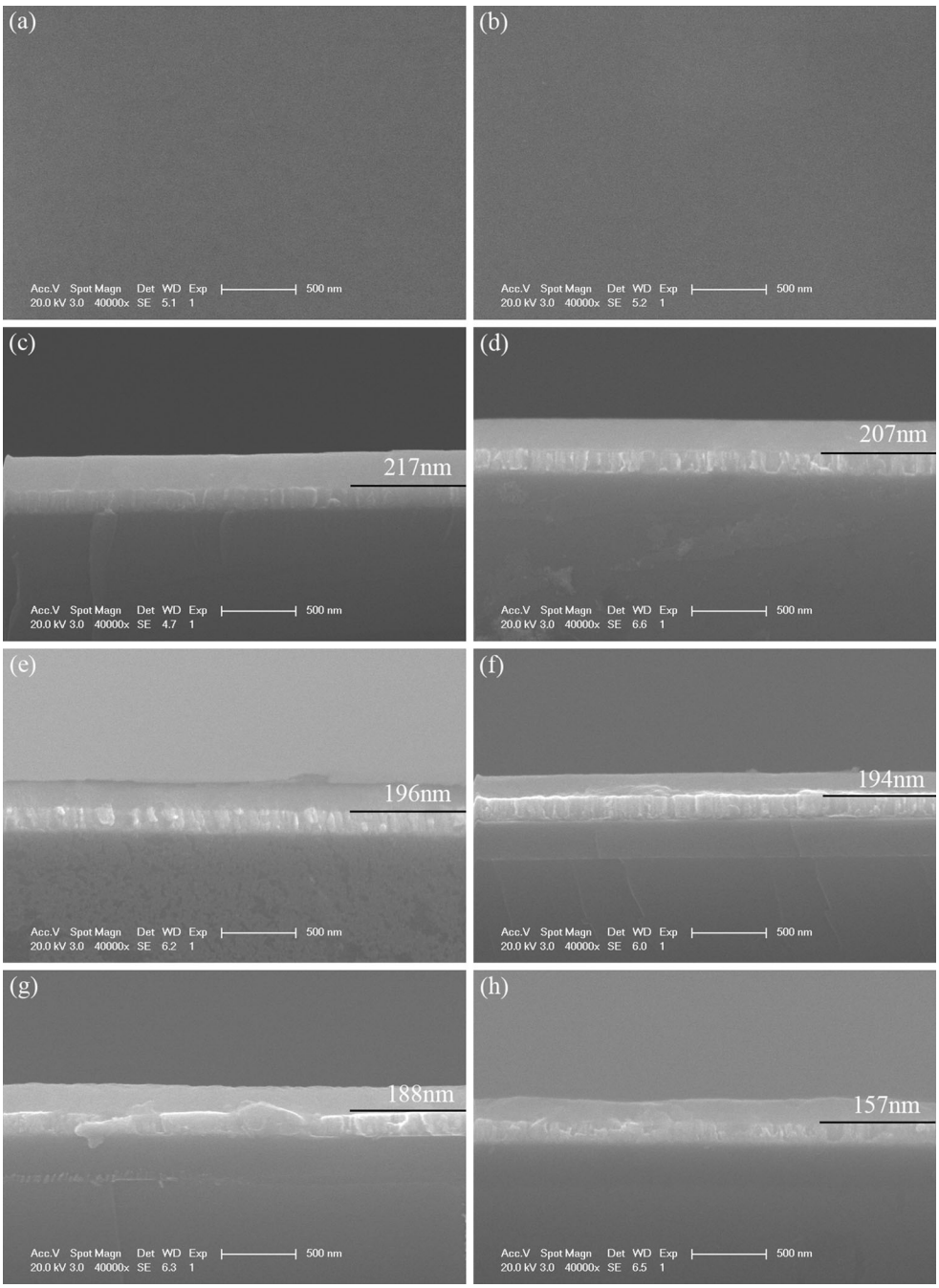

Fig. 2 Surface FESEM images of Al_2O_3 (**a**) and AM-33.3 (**b**) films deposited on Pt/Ti/SiO_2/Si substrates; cross-section FESEM images of Al_2O_3 (**c**), AM-0.5 (**d**), AM-2 (**e**), AM-7.7 (**f**), AM-10 (**g**) and AM-33.3 (**h**) films on Pt/Ti/SiO_2/Si substrates

permittivity of free space, ε_r the optical dielectric constant of the films, and E_I the trap ionization energy. Schottky barrier forms at the electrode/films interface with a low concentration of charge carriers, and the leakage current is described by the following equation [12]:

$$J_S = A^* T^2 \exp -[(\phi_b - \beta_S E^{1/2})/kT], \quad (2)$$

where $\beta_s = (q^3/4\pi\varepsilon_0\varepsilon_r)^{1/2}$, A^* is the Richardson contant and ϕ_b is the Schottky barrier height. If the PF or SE are the dominant leakage mechanism, plots of $\mathrm{Ln}(J/E)$-$E^{1/2}$ and $\ln(J/T^2)$-$E^{1/2}$ will show straight line fits to the data. Figure 3b, c show that the data satisfy the PF and SE equations. The slopes of the fits provide an estimate of the

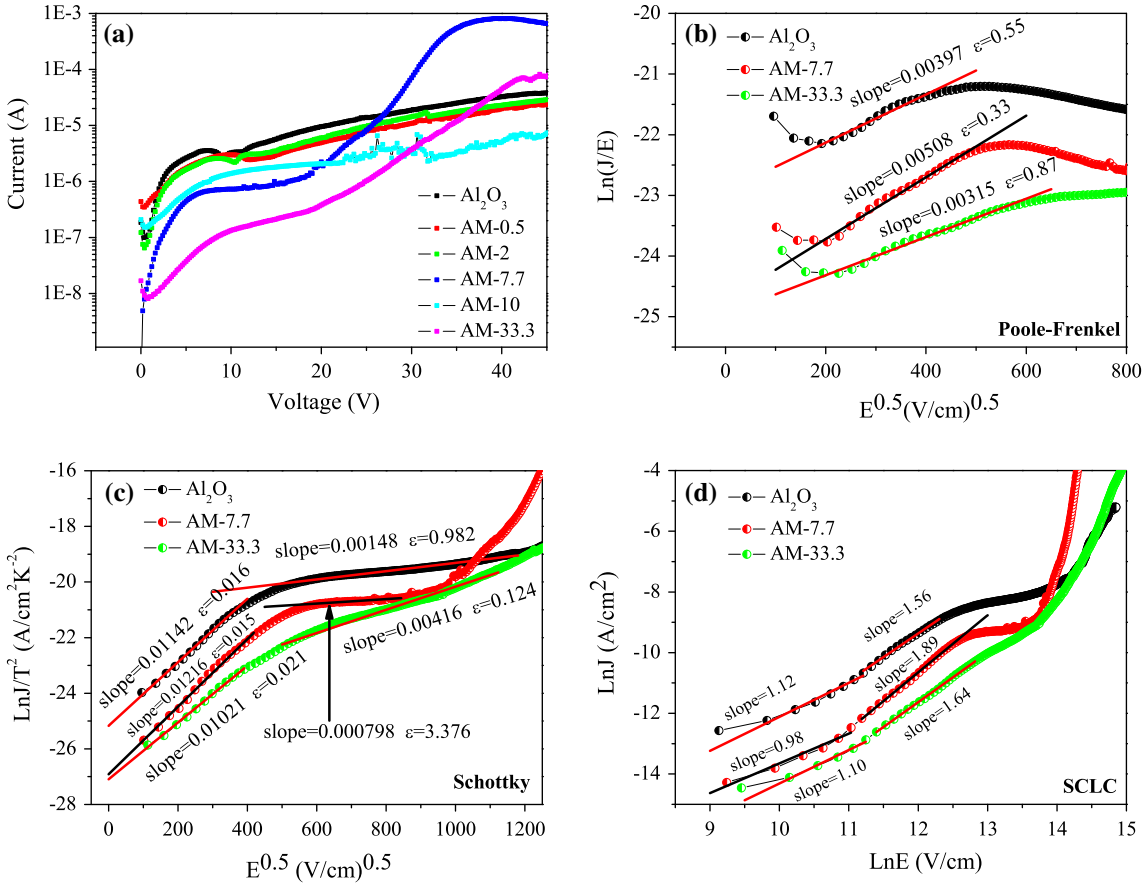

Fig. 3 *I-V* Plots (**a**) of $Al_{1-x}Mg_xO_y$ films, Ln(J/E)-$E^{1/2}$ plots (**b**), ln(J/T^2)-$E^{1/2}$ plots (**c**) and ln(J)-ln(E) plots (**d**) for Al_2O_3, AM-7.7 and AM-33.3 films

optical dielectric constant. The refractive index (n) of amorphous Al_2O_3 and $MgAl_2O_4$ films is 1.5 [13], 1.61 [14], respectively. The dielectric constant can be found as n^2 (there is no report about the refractive index of $MgAl_{12}O_{19}$). The extracted values of ε_r in PF are smaller than the expected values, while the calculated values of ε_r in SE lie clearly outside this range in lower electric field (<16 MV/m). A distinct difference occurs in the values under higher electric field (>36 MV/m), they are 0.98, 3.38 and 0.12 for Al_2O_3, AM-7.7 and AM-33.3 films, respectively.

When the injected electrons are trapped in the films and form the space charge, the internal field is dominated by the space charge. The leakage current J is expected to display a power-law dependence on voltage [15, 16],

$$J = C\frac{V^n}{d^m}, \tag{3}$$

where C, n and m are arbitrary constant, d the thickness of films, and V the applied voltage. The slopes extracted by $\ln(J) - \ln(E)$ plots of all films are around 1 under lower electric field (<10 MV/m), which is consistent with the expected value of 1 for the Ohmic conduction mechanism. The above result suggests that the ohmic conduction is dominant at lower electric field in all the films. Under higher electric field (>10 MV/m), the extracted values are 1.56, 1.89 and 1.64 for Al_2O_3, AM-7.7 and AM-33.3 films, respectively, which are very close to 2 for the SCLC conduction. Therefore, the leakage current in such films cannot be purely SCLC since the value of power-law index n deviates slightly from 2. On the whole, the Ohmic conduction dominates the leakage current of Al_2O_3, AM-7.7 and AM-33.3 films under lower electric field, while the SCLC and SE, and even other conduction mechanism, could co-exist under higher electric field.

Actually weak-spot breakdown occurs prior to the intrinsic breakdown. Therefore the dielectric strength is highly sensitive to the micro-defects of the films, such as pinholes and micro-cracks [17]. In this study, the weibull distribution was employed to investigate the dielectric strength of the films. The breakdown is usually characterized by the abrupt increase of the leakage current. Figure 4 illustrates the Weibull distribution of the breakdown voltage of $Al_{1-x}Mg_xO_{3-\delta}$ films. As shown in Fig. 4, the dates show a relatively good linearity. The calculated breakdown

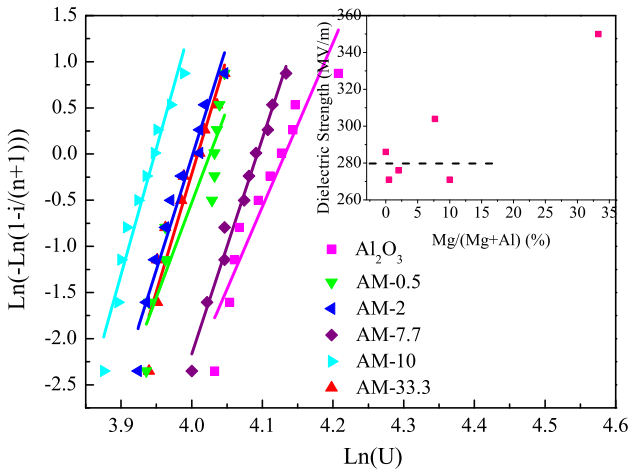

Fig. 4 Weibull plots of breakdown voltage of $Al_{1-x}Mg_xO_{3-\delta}$ films. Inset: dielectric strength of $Al_{1-x}Mg_xO_{3-\delta}$ films

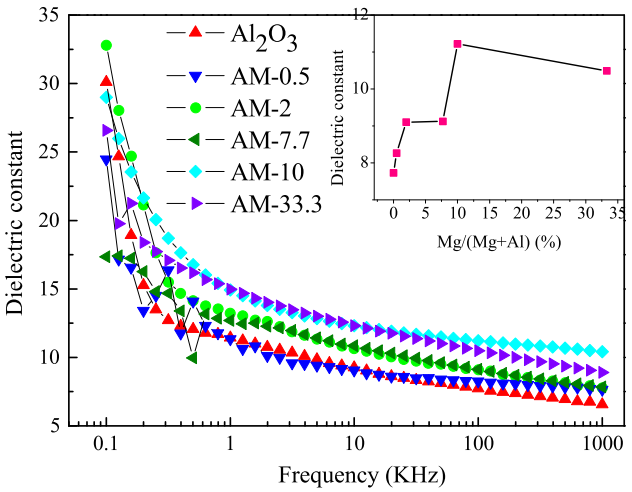

Fig. 5 Frequency dependence of dielectric constant of $Al_{1-x}Mg_xO_{3-\delta}$ films, Inset: dielectric constant of $Al_{1-x}Mg_xO_{3-\delta}$ films at 100 kHz

voltage of Al_2O_3, AM-0.5, AM-2, AM-7.7, AM-10 and AM-33.3 films are 62, 56, 54, 59, 51 and 55 V, respectively. The dielectric strengthen is defined as the breakdown voltage divided by the physical thickness of the insulating materials. As shown in the inset of Fig. 4, the dielectric strengthen of Al_2O_3, AM-0.5, AM-2, AM-7.7, AM-10 and AM-33.3 films are 286, 271, 276, 304, 271 and 350 MV/m, respectively.

Compared with undoped Al_2O_3 films, the AM-0.5, AM-2 and AM-10 films have a slightly lower dielectric strength, which could be attributed to the increasing charge traps with Mg addition. For Mg-doped Al_2O_3 films, the defect reaction can be described as follows:

$$2MgO \xrightarrow{Al_2O_3} 2Mg'_{Al} + 2O_o + V_O^{\cdot\cdot}, \quad (4)$$

The Mg addition can effectively motivate the formation of oxygen vacancy. Moreover, it has been proved that there are also a large amount of oxygen vacancies in the amorphous Al_2O_3 films [18]. The increasing oxygen vacancies in the films are able to capture electrons and play as electron traps [18, 19]. When the electrons trap amount exceeds a critical density, the films will lose its local dielectric integrity due to breakdown [20]. However, the AM-7.7 and AM-33.3 films possess higher dielectric strength surprisingly, which could be closely related to the potential magnetoplumbite and spinel phase within the short-range scope, respectively.

Figure 5 shows the frequency dependence of dielectric constant of $Al_{1-x}Mg_xO_{3-\delta}$ films. It is observed that the frequency dependence can be divided into two segments. At the lower frequency (<10 kHz), the large fluctuation of the dielectric constant can be ascribed to DC-conductivity. At the frequency above 10 kHz, the dielectric constant remains almost frequency independent. As shown in the inset of Fig. 5, in general, the dielectric constant increases with the addition content of magnesium except for the AM-7.7 and AM-33.3 films.

4 Conclusions

Highly homogeneous and dense $Al_{1-x}Mg_xO_{3-\delta}$ films have been prepared by sol–gel technology. The $Al_{1-x}Mg_xO_{3-\delta}$ (x = 0, 0.5, 2 and 10 %) films display the similar shapes in the I–V curves. There is no obvious change in the leakage current of $Al_{1-x}Mg_xO_{3-\delta}$ (x = 0, 0.5, 2 and 10 %) films, except the leakage current of the AM-10 films is slightly smaller than that of the updoped Al_2O_3 films. But for the AM-7.7 and AM-33 films, the shape of I-V curves is different from the above four kinds of films. The leakage current of AM-7.7 films increases sharply when the applied voltage is higher than 25 V, and the leakage current is significantly higher than the others. As for the AM-33 films, the leakage current almost grows linearly throughout the applied voltage. Under lower electric field, the Ohmic conduction dominates the leakage current of Al_2O_3, AM-7.7 and AM-33.3 films, while the SCLC and SE, and even other conduction mechanisms together, could be the dominant conduction mechanism under higher electric field. Compared with the undoped Al_2O_3 films, the $Al_{1-x}Mg_xO_{3-\delta}$ (x = 0.5, 2 and 10 %) films have a slightly lower dielectric strength, which could be related to the increasing electron traps with Mg addition. While the AM-7.7 and AM-33.3 films possess higher dielectric strength than the undoped Al_2O_3 films. It is expected that the abnormal behaviors of samples AM-7.7 and AM-33.3 could be related to the potential $MgAl_{12}O_{19}$ and $MgAl_2O_4$ phase.

Acknowledgments This work is supported by the Ministry of Science and Technology of China through 973-project (Grant Number 2015CB654601), International Science & Technology Cooperation Program of China (Grant Number 2013DFR50470) and National Science Foundation of China (Grant Number 51272177).

References

1. I. Piwoński, K. Soliwoda, Ceram. Int. **36**, 47 (2010)
2. R. Al-Bayer, A. Zihlif, B. Lahlouh, Z. Elimat, G. Ragosta, J. Mater. Sci. Mater. Electron. **24**, 2866 (2013)
3. H.C. Lin, P.D. Ye, G.D. Wilk, Appl. Phys. Lett. **87**, 182904 (2005)
4. M.W. Yao, J.W. Chen, P.F. Yang, W. Shan, B.F. Hu, X. Yao, Ferroelectrics **455**, 21 (2013)
5. R.B.V. Dover, Appl. Phys. Lett. **74**, 3041 (1999)
6. H. Fujikawa, Y. Taga, J. Appl. Phys. **75**, 2538 (1994)
7. K.M.A. Salam, H. Fukuda, S. Nomura, J. Appl. Phys. **93**, 1169 (2003)
8. W.S. Lau, T.S. Tan, P. Babu, N.P. Sandler, Appl. Phys. Lett. **90**, 112903 (2007)
9. M.W. Yao, R.H. Xiao, Y. Peng, J.W. Chen, B.F. Hu, X. Yao, J. Sol Gel Sci. Technol. **74**, 39 (2015)
10. B.F. Hu, M.W. Yao, P.F. Yang, W. Shan, X. Yao, Ceram. Int. **39**, 7613 (2013)
11. J.C. Jackson, T. Robinson, O. Oralkan, D.J. Dumin, J. Electrochem. Soc. **145**, 1033 (1998)
12. S.K. Sahoo, R.P. Patel, C.A. Wolden, Appl. Phys. Lett. **101**, 142903 (2012)
13. P. Zou, M.W. Yao, J.W. Chen, Y. Peng, X. Yao, Ceram. Int. **42**, 4120 (2016)
14. I.V. Afanasyev-Charkin, D.W. Cooke, M. Ishimaru, B.L. Bennett, V.T. Gritsyna, J.R. Williams, K.E. Sickafus, Opt. Mater. **16**, 397 (2001)
15. L.Y. Wang, W. Ren, P. Shi, X.Q. Wu, J. Appl. Phys. **115**, 034103 (2014)
16. J.C. Shin, C.S. Hwang, H.J. Kim, S.O. Park, Appl. Phys. Lett. **75**, 3411 (1999)
17. H. Kim, T. Troczynski, Ceram. Int. **33**, 333 (2007)
18. T.V. Perevalov, O.E. Tereshenko, V.A. Gritsenko, V.A. Pustovarov, A.P. Yelisseyev, C. Park, J.H. Han, C. Lee, J. Appl. Phys. **108**, 013501 (2010)
19. D. Liu, S.J. Clark, J. Robertson, Appl. Phys. Lett. **96**, 032905 (2010)
20. K. Ganesan, S. Ilango, M. Shanmugam, M.F. Baroughi, M. Kamruddin, A.K. Tyagi, Curr. Appl. Phys. **13**, 1865 (2013)